Impact Factor:					
	ISRA (India) = 6.317	SIS (USA) = 0.912	ICV (Poland) = 6.630
	ISI (Dubai, UAE) = 1.582	РИНЦ (Russia) = 3.939	PIF (India) = 1.940
	GIF (Australia) = 0.564	ESJI (KZ) = 8.771	IBI (India) = 4.260
	JIF = 1.500	SJIF (Morocco) = 7.184	OAJI (USA) = 0.350

SOI: 1.1/TAS DOI: 10.15863/TAS

International Scientific Journal

Theoretical & Applied Science

p-ISSN: 2308-4944 (print) **e-ISSN:** 2409-0085 (online)

Year: 2022 **Issue:** 08 **Volume:** 112

Published: 03.08.2022 **http://T-Science.org**

Issue Article

Lamiaa Abd Alhussein Ward
University of Kufa
Department of Physics, Faculty of Science, Najaf, Iraq

Abbas H. Abo Nasria
University of Kufa
Department of Physics, Faculty of Science, Najaf, Iraq
abbas.abonasiriya@uokufa.edu.iq

THEORETICAL INVESTIGATION OF A P-DOPED(Al_8C_9) MONOLAYER FOR DETECTING TOXIC GAS MOLECULES SELECTIVELY

Abstract: *The B3LYP functional and 6-31G (d, p) basis set calculations were used to explore the sensitive features of microscopic toxic gas molecules (CO, NO, SO, HCN) on a P-doped(Al_8C_9) monolayer. These gases are a key cause of environmental degradation. Adsorption energy, adsorption distance, and charge transfer parameters were used to find the best adsorption point among tow adsorption sites: C, and Bridge. These (CO, NO, SO, and HCN) gas molecules are adsorbed on a P-doped(Al_8C_9) monolayer, according to the adsorption energy and electron localization function data. Our findings further show that there is a significant amount of charge transfer between SO and NO molecules and the P-doped(Al_8C_9) monolayer after adsorption. This means that a P-doped(Al_8C_9) monolayer is more vulnerable to NO and SO adsorption than virgin or doped graphene. Furthermore, small gas molecule adsorption will alter the bandgap and work function of the P-doped(Al_8C_9) monolayer to varying degrees. Our research will provide theoretical and practical applications.*

Key words: *DFT. B3LYP, aluminum carbon, gas adsorption, HOMO, LUMO.*

Language: *English*

Citation: Ward, L. A., & Abo Nasria, A. H. (2022). Theoretical investigation of a P-doped(Al_8C_9) monolayer for detecting toxic gas molecules selectively. *ISJ Theoretical & Applied Science, 08 (112)*, 177-184.

Soi: http://s-o-i.org/1.1/TAS-08-112-13 ***Doi***: crossref https://dx.doi.org/10.15863/TAS.2022.08.112.13

Scopus ASCC: *3100.*

Introduction

Because of their fascinating optoelectronic features and excellent thermal and mechanical stability, semiconductors have drawn a lot of attention in the last decade[1], [2]. They are currently widely utilized in efficient short wavelength light-emitting diodes (LEDs) (blue and ultraviolet), room-temperature laser diodes, and field-effect transistors[3], [4]. Aluminum nitride (AlN) has a higher thermal conductivity at low temperatures, higher thermal stability, low thermal expansion coefficient, high dielectric breakdown strength, good mechanical strength, excellent chemical stability, and nontoxicity than the other semiconductors nitride and carbide[5], [6]. The electrical characteristics of AlN materials are affected by chemical species adsorption, which is of fundamental interest and importance in the creation of prospective electronic sensors[7][8]. The charge transfers between the AlN and AlC sheet and the adsorbate can change the carrier density in semiconducting sheets,[9] which has a big impact on the material's electrical conductance. Several groups have proposed the use of AlN and AlC sheets as promising gas sensors based on these findings[10]. In the presence of NH3, we recently shown that an AlN sheet can detect low concentrations of NO2[7]. Nine out of ten people live in areas where air pollution levels exceed WHO guidelines, and this is due to air pollution, toxic gases like [NO, SO, HCN, CO] [8][11], found in many chemical and industrial plants, including natural gas processing and utilization, wastewater treatment, and semiconductor manufacturing, not to mention pollution-induced ozone layer depletion. Some poisonous gases aren't

visible, can't be smelled, or don't have a noticeable effect right away[12][13]. As a result, without the use of tools or machines, It is impossible to identify them only through the use of human senses. As a result, gas sensors were required to detect harmful chemicals and monitor air pollution. To address these difficulties, scientists must explore for materials that consume little energy, respond quickly, and are sensitive to gases[11]. As a result, we discovered that two-dimensional monolayers have a large surface area and are part of a new class of sensors. Monolayer graphene has extraordinary features.[14][15] As well as constructing ultra-sensitive sensors based on theoretical and practical research

II. Computational details

To forecast electronic characteristics, Eads, and equilibrium geometries, all calculations were performed using density functional theory (DFT) and dispersion corrected B3LYP functional[16] with 6-31G(d) basis set as implemented in Gaussian 09 package suite of programs[17][18]. On a single-layer of AlC sheet (consisting of 9 Al, 8 C and 1P atoms arranged in hexagonal rings), geometry optimization was accomplished. Figure 1 shows a partial structure of an optimized sheet. Hydrogen atoms saturated the dangling bonds near the sheet's border, decreasing boundary effects. Eq. 1 was used to identify the Eads of the molecules on the sheet's surface. To do complete geometric optimizations of the absorption impact of single-layer AlC molecules on CO, SO, NO, and HCN gas. The chemical potential or Fermi energy (E_F) of the complexes was obtained, as shown below[19][20]:

$$E_F = (EHOMO + ELUMO)/2 \quad (1)$$

Where:

-EHOMO: the energy of the higher occupied molecular orbital.

-ELUMO: the energy of the lower unoccupied molecular orbital.

In addition, the energy gap in the energy levels (for example) of the system is recognized as follows[21]:

$$E_g = E_{LUMO} - E_{HOMO} \quad (2)$$

The adsorption energy (E_{ads}) was calculated using the following pretty close expression[22][23]:

$$E_{ads} = E_{(COMPLEX)} - (E_{(MOLECULE)} + E_{(GAS)}) \quad (3)$$

Where:

- $E_{(COMPLEX)}$: The actual molecule energy with gas adsorption.
- $E_{(MOLECULE)}$: The total energy without absorption of the studied molecule.
- $E_{(GAS)}$: Gas molecule's total energy[24][19]. The charge transfers between the sheet and the adsorbed molecules was calculated using natural bond orbital (NBO) analysis.

III. RESULTS AND DISCUSSIONS

1. Adsorption configurations

As shown in Fig. 1, the P- doped(Al_8C_9) cone contains a single layer. Eight aluminum atoms and nine carbon atoms, one aluminum atom replaced with one phosphorus atom, in the P- doped(Al8C9) cone, there are two types of adsorption sites. The distance between the P- doped(Al_8C_9) substrate and the gas molecules are initially set to 2.5 Å. Furthermore, the original orientation of the gas molecule is perpendicular to the substrate. Because gas molecules absorb in a variety of configurations, a variety of insertion geometries must be considered, (CO, SO, NO, and HCN) gas molecule at a distance from 2.5 Å over P atom and bridge. One of the triatomic original orientations (HCN) is on the other hand taken into account. The carbon atom in the HCN molecular is on the top of the P-C in the parallel direction, in the second direction while the C atoms of HCN point towards the bridge in P-C layer in the same direction. The entire system can then relax completely. The compounds' absorption energies will be used to determine how they interact with the P- doped(Al_8C_9) layer. Based on the equation. The lower the E_{ad} value, the greater the adsorption of gas molecules onto P-doped(Al_8C_9). The most energy-appropriate adsorption designs are chosen for further research.

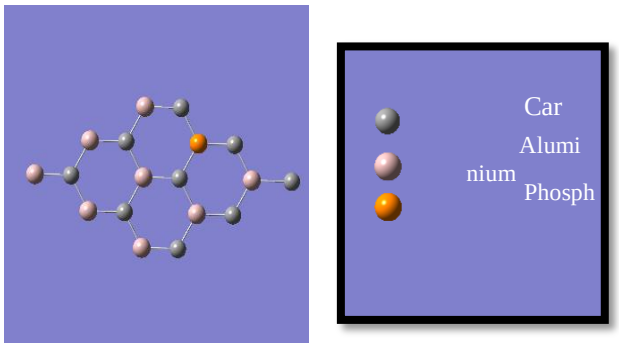

Fig. 1. Geometric structures of P-doped(Al_8C_9) cone.

The adsorption energy (E_{ads}), electronic properties of the investigated molecules such as HOMO, LUMO, total energy (E_{tot}), energy gap (E_g), and Fermi Energy (E_F) were determined after improving the geometry, as shown in Table 1.

Table1: Structural and electronic properties of P- doped(Al_8C_9) cone.

Model	Site	LOMO	HOMO	E_g eV	E_F e.v
CO	Bridge	-0.12443	-0.19435	1.902616	-4.33721
	$P_{(atom)}$	-0.12409	-0.19444	1.914317	-4.33381
SO	Bridge	-0.13119	-0.19565	1.754042	-4.44687
	$P_{(atom)}$	-0.12885	-0.19399	1.772546	-4.39245
NO	Bridge	-0.17722	-0.19573	0.503682	-5.07423
	$P_{(atom)}$	-0.17444	-0.19146	0.463137	-4.97831
HCN	Bridge	-0.11132	-0.19029	2.148878	-4.1036
	$P_{(atom)}$	-0.14954	-0.20739	1.574175	-4.85627

Table 1 summarizes the adsorption energies of different gas molecules thought about in this work on P- doped(Al_8C_9). We ignore the different orientations of adsorbed gas molecules since we are only interested in the influence of gas adsorption on the electrical structure of the P- doped(Al_8C_9) cone. On the other hand, electronic structure is analyzed irrespective of direction and adsorption sites.

Table 2: Adsorption energies, adsorption height, and transfer charges for adsorption configurations.

Model	Site	D °A	r °A	E_{ad} eV	Q |e|
CO	Bridge	2.13989	1.86	-0.4518	+0.01
	$P_{(atom)}$	2.14152	1.86	-0.4543	-0.28
SO	Bridge	1.82936	1.85	-0.696	+0.039
	$P_{(atom)}$	1.1446	1.85	-0.690	-0.003
NO	Bridge	1.34717	1.83	-0.645	-0.048
	$P_{(atom)}$	1.2929	1.83	-1.855	-0.026
HCN	Bridge	2.11191	1.86	-0.1	-0.002
	$P_{(atom)}$	2.14643	1.86	-0.3	-0.008

3.2.1. (CO) Adsorption on P- doped(Al_8C_9) cone.

CO gas molecule adsorption on the P-doped(Al_8C_9) Nano-cone is examined. Figure 8 shows the P- doped(Al8C9)-CO complex's most stable adsorption configuration. The CO molecule is positioned perpendicular to the P-doped(Al_8C_9) plane at different positions, first on the P atom, and the P-C bridge, (-0.4518) and (-0.4543) are the adsorption energies, respectively. CO and P- doped(Al8C9) have a mean atom-atom distance (C-P bond length) of 2.14152, which is greater than the C-P dimer bond length (1.86), and the atom-atom distance between CO and the P-C bridge is 2.13989, which is greater than the length of the P-C dimer bond (1.86). CO physically adsorbs on the P-doped(Al_8C_9) layer, according to these findings.

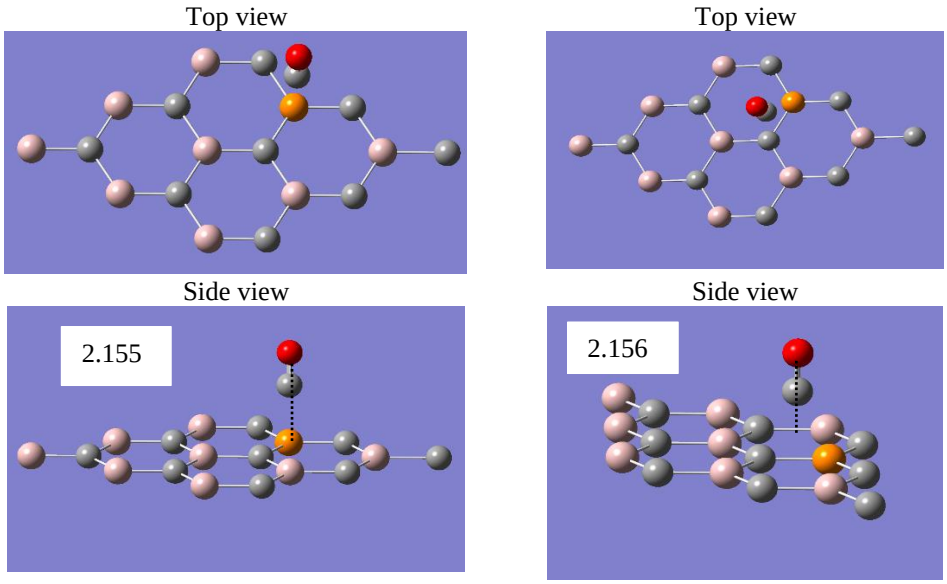

Fig.2: Top and side views of the most stable combinations (a) P-atom (b) the bridge, CO adsorbed on the top site of P-doped(Al_8C_9)

3.2.2. (SO) Adsorption on P-doped(Al_8C_9) Nano-cone.

The adsorption of SO gas molecules on a Nano-cone of P-doped(Al8C9) is investigated. Figure (9) shows the SO-P-doped(Al8C9) complex's most stable adsorption structure. At certain points, the SO molecule is perpendicular to the P-doped(Al8C9) plane, namely the atom, and the P-C bridge. Adsorption energies are -0.696, -0.690, respectively for P-doped(Al8C9). The mean atom-atom distance (S-P bond length) between SO and P-doped(Al8C9) is 1.1446, which is less than the sum of covalent atomic radii of S-P (1.85 Å), and the atom-atom distance between SO and the S-P bridge is 1.82936, which is less than the length of the P-C dimer bond (1.85). These findings indicate that SO is chemically adsorbent.

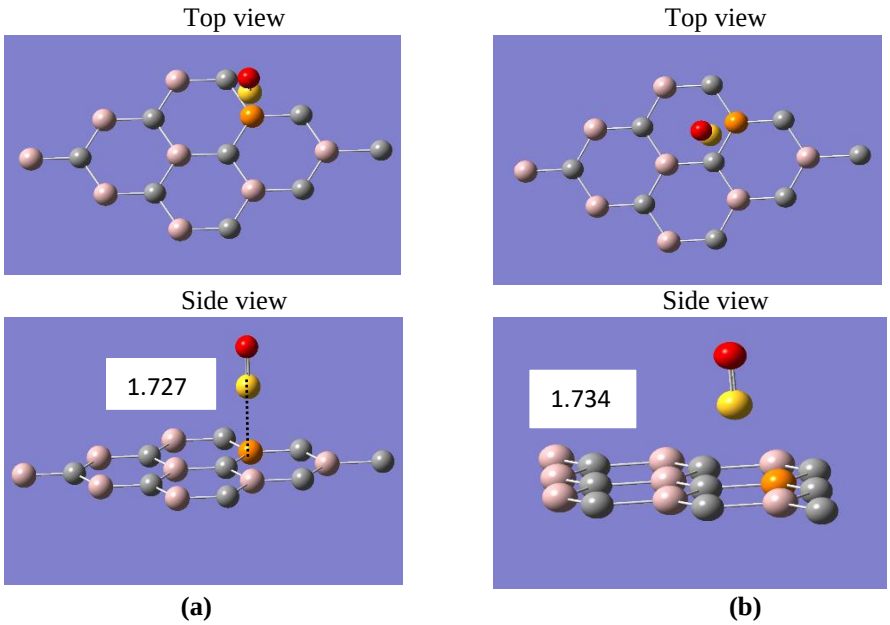

Fig.3: Top views and side views of most stable configurations of (a) P-atoms, (b)bridge, SO adsorbed on the top site of P-doped(Al_8C_9)

3.2.1. (NO) Adsorption on P-doped(Al_8C_9) Nano-cone

When NO is exposed to the P-doped(Al_8C_9) layer, it takes an oblique direction in relation to the P-doped(Al_8C_9) level, as shown in Fig. 10. The N atom

of the NO atom indicates the C atom in the P-doped(Al_8C_9). the atom's and P-C bridge's adsorption energies are -0.645 and -1.855, respectively, for P-doped(Al_8C_9). The mean atom-atom distance (N-P bond length) between NO and P-doped(Al_8C_9) is 1.32613, which is less than the N-P dimer bond length (1.51), and the minimum distance of atom-atom from NO to the bridge Al-C is 1.37221, which is less than the length of the N-P dimer bond (1.51). These findings indicate that the NO is chemically adsorbing on the P-doped(Al_8C_9) layer.

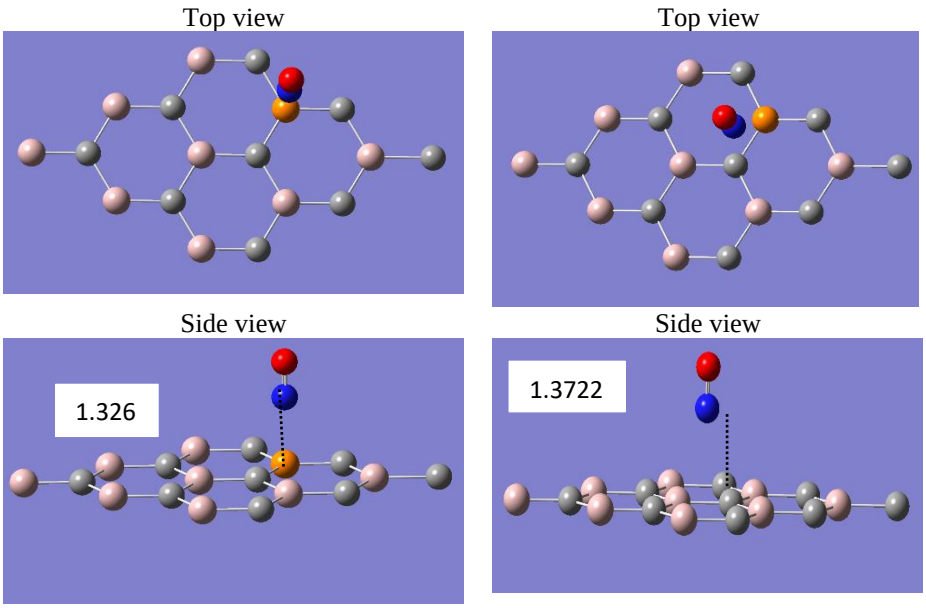

Fig.4: Top views and side views of most stable configurations of (a) P-atoms, (b)bridge, NO adsorbed on the top site of P-doped(Al_8C_9)

3.2.2. (HCN) Adsorption on P-doped(Al_8C_9) Nano-cone

The adsorption of HCN on BN Nano-cones is more difficult than the adsorption of the other molecules discussed previously. Parallel to P-doped(Al_8C_9) the gas lies above the P-doped(Al_8C_9) Nano-cone, the carbon atom in HCN molecule placed above the C in the P-doped(Al_8C_9), and on the bridge between P-C as shown in fig.11. the adsorption energies are -0.114, -0.264 eV, respectively, the mean atom-atom distance (C-P) between HCN and P-doped(Al_8C_9) is 2.146, which is larger than the C-P dimer bond (1.54), and the distance atom-bridge between HCN and P-doped(Al_8C_9) is 2.111, which is larger than the C-C dimer bond (1.54). These results show that the HCN is physically adsorbed on P-doped(Al_8C_9) Nano-cone.

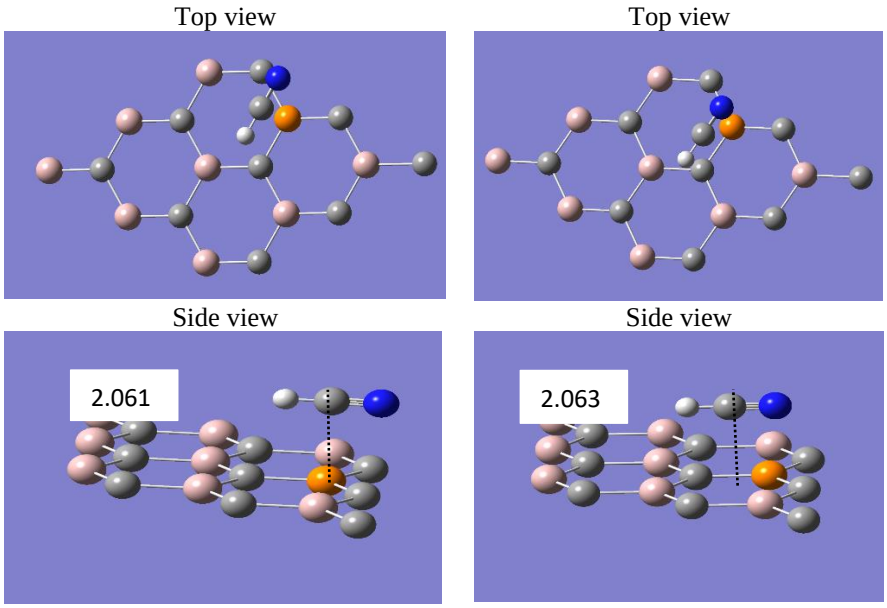

Fig.5: Top views and side views of most stable configurations of (a) P-atom, (b) bridge, HCN adsorbed on the top site of P-doped(Al_8C_9)

3.2.3. The electronic structure of the P-doped(Al_8C_9) Nano-cone

We can learn about electron states at the Fermi surface as well as transported electrons since the HOMO and LUMO orbits are near to the Fermi plane. Figure 12 shows the distribution of the HOMO and LUMO orbitals. The electron cloud distribution in these two orbits is concentrated at the edge of P-doped(Al_8C_9) Nano-cone, as we discovered,

Model	Site	HOMO		LOMO
CO	Bridge	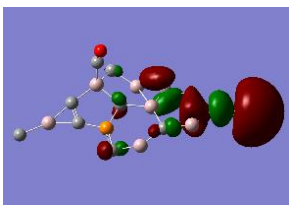	E_g eV 1.34968	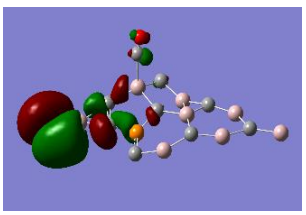
	$P_{(atom)}$	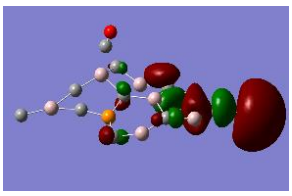	E_g eV 1.62043	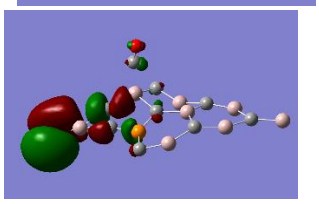
SO	Bridge	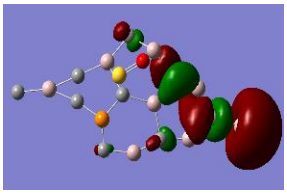	E_g eV 1.33907	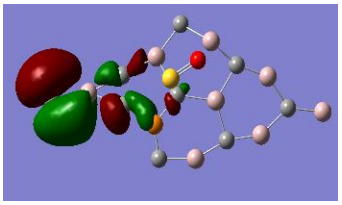
	$P_{(atom)}$	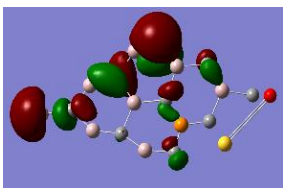	E_g eV 1.62724	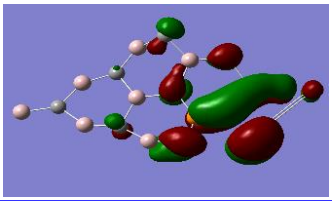

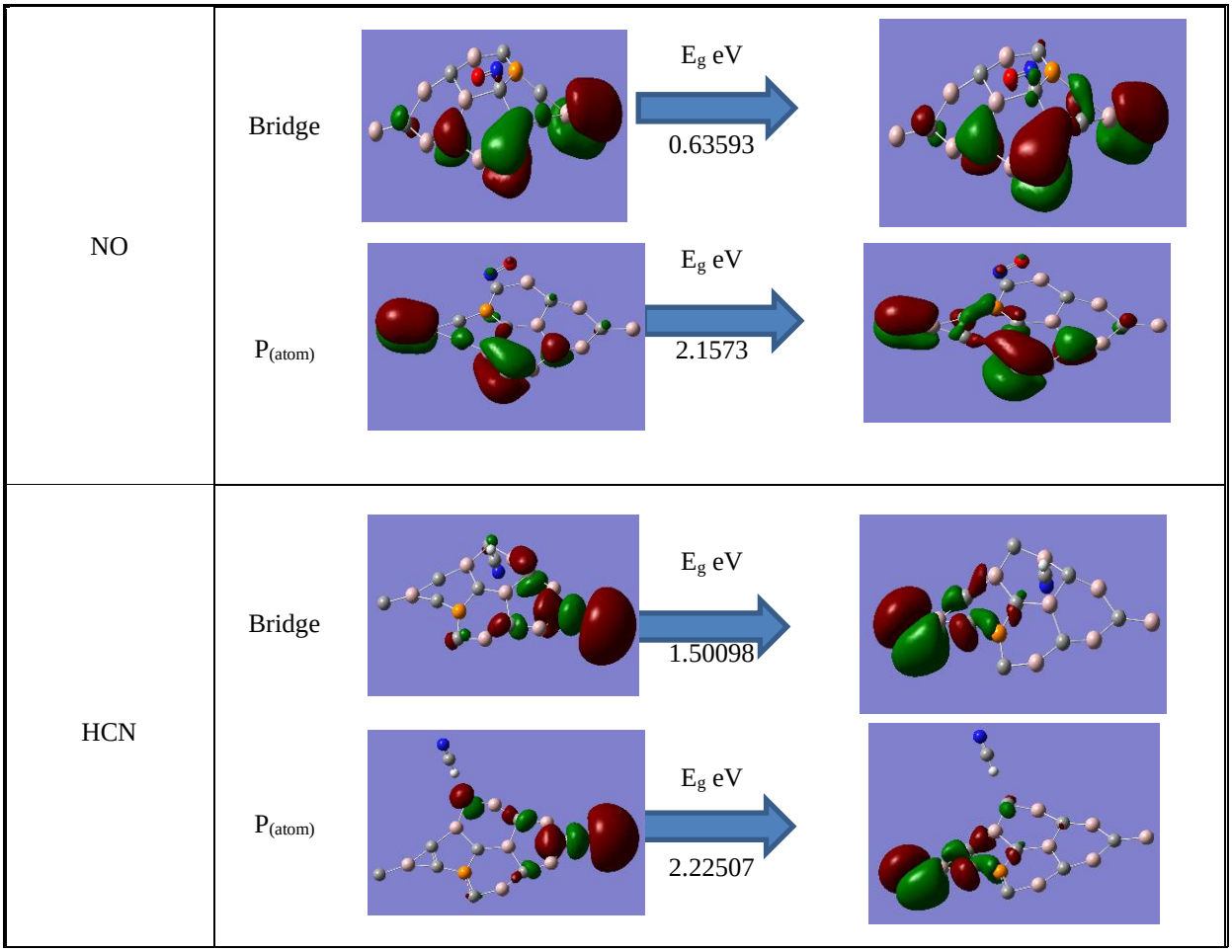

Fig.6. The electronic structure of the P-doped(Al_8C_9) Nano-cone

1.6 CONCLUSION

Finally, the DFT theoretical findings demonstrate that P-doped(Al_8C_9) monolayers exhibit a wide range of behaviors when exposed to normal and contaminated gas molecules. The P-doped(Al_8C_9) monolayer has a higher affinity for CO, SO, NO, and HCN molecules. The chemical adsorption character of SO, NO, adsorptions can be readily recognized with broad Ead, charge transfer. For HCN and CO, there is also physical adsorption. As a result, the P-doped(Al_8C_9) monolayers sheet is a likely candidate for gas sensors for SO, CO, NO, and HCN.

References:

1. Beheshtian, J., Kamfiroozi, M., Bagheri, Z., & Ahmadi, A. (2011). "Computational study of CO and NO adsorption on magnesium oxide nanotubes," *Phys. E Low-Dimensional Syst. Nanostructures*, vol. 44, no. 3, pp. 546-549, doi: 10.1016/j.physe.2011.09.016.
2. Beheshtian, J., Peyghan, A. A., & Bagheri, Z. (2012). "Quantum chemical study of fluorinated AlN nano-cage," *Appl. Surf. Sci.*, vol. 259, pp. 631-636, Oct. 2012, doi: 10.1016/J.APSUSC.2012.07.088.
3. Vurgaftman, I., Meyer, J. R., & Ram-Mohan, L. R. (2001). "Band parameters for III-V compound semiconductors and their alloys," *J. Appl. Phys.*, vol. 89, no. 11 I, pp. 5815-5875, doi: 10.1063/1.1368156.
4. Mourad, D. (n.d.). *"Tight-binding branch-point energies and band offsets for cubic InN, GaN, AlN and AlGaN alloys."*

5. Zhang, Y. H., et al. (2009). "Improving gas sensing properties of graphene by introducing dopants and defects: A first-principles study," *Nanotechnology*, vol. 20, no. 18, doi: 10.1088/0957-4484/20/18/185504.
6. Torres, I., Mehdi Aghaei, S., Rabiei Baboukani, A., Wang, C., & Bhansali, S. (2018). "Individual Gas Molecules Detection Using Zinc Oxide-Graphene Hybrid Nanosensor: A DFT Study," C, vol. 4, no. 3, p. 44, doi: 10.3390/c4030044.
7. Hadipour, N. L., Ahmadi Peyghan, A., & Soleymanabadi, H. (2015). "Theoretical study on the Al-doped ZnO nanoclusters for CO chemical sensors," *J. Phys. Chem. C*, vol. 119, no. 11, pp. 6398-6404, Mar. 2015, doi: 10.1021/JP513019Z.
8. Safari, F., Moradinasab, M., Fathipour, M., & Kosina, H. (2018). "Adsorption of the NH_3, NO, NO_2, CO_2, and CO gas molecules on blue phosphorene: A first-principles study," *Appl. Surf. Sci.*, vol. 464, no. September 2018, pp. 153-161, doi: 10.1016/j.apsusc.2018.09.048.
9. G, Z.A., & Nasria, A. H. A. (2021). "DFT investigation of BN monolayer as a gas sensor for the detection of SO, SO_2NO, and NO_2 gases," vol. 63, no. 06, pp. 7681-7693.
10. Dai, J., Wu, X., Yang, J., & Zeng, X. C. (2014). "AlxC monolayer sheets: Two-dimensional networks with planar tetracoordinate carbon and potential applications as donor materials in solar cell," *J. Phys. Chem. Lett.*, vol. 5, no. 12, pp. 2058-2065, doi: 10.1021/jz500674e.
11. Shlaka, J. A., & Abo Nasria, A. H. (2020). "Density functional theory study on the adsorption of AsH_3 gas molecule with monolayer $(AlN)_{21}$ (including pristine, C, B doped and defective aluminium nitride sheet)," *IOP Conf. Ser. Mater. Sci. Eng.*, vol. 928, no. 7, pp. 1-16, doi: 10.1088/1757-899X/928/7/072082.
12. Zhao, Z., Yong, Y., Zhou, Q., Kuang, Y., & Li, X. (2020). "Gas-Sensing Properties of the SiC Monolayer and Bilayer: A Density Functional Theory Study," *ACS Omega*, vol. 5, no. 21, pp. 12364-12373, doi: 10.1021/acsomega.0c01084.
13. Abed Al-Abbas, S. S., Muhsin, M. K., & Jappor, H. R. (2019). "Two-dimensional GaTe monolayer as a potential gas sensor for SO2 and NO2 with discriminate optical properties," *Superlattices Microstruct.*, vol. 135, p. 106245, doi: 10.1016/j.spmi.2019.106245.
14. Beheshtian, J., Kamfiroozi, M., Bagheri, Z., & Ahmadi, A. (2011). "Computational study of CO and NO adsorption on magnesium oxide nanotubes," *Phys. E Low-Dimensional Syst. Nanostructures*, vol. 44, no. 3, pp. 546-549, Dec. 2011, doi: 10.1016/J.PHYSE.2011.09.016.
15. Vo, D. D., et al. (2020). "Janus monolayer PtSSe under external electric field and strain: A first principles study on electronic structure and optical properties," *Superlattices Microstruct.*, vol. 147, no. June, 2020, doi: 10.1016/j.spmi.2020.106683.
16. (2022). *"Gaussian 09 Citation. Gaussian.com."* Retrieved Jun. 03, 2022 from https://gaussian.com/g09citation/
17. Schmidt, M. W., et al. (1993). "General atomic and molecular electronic structure system," *J. Comput. Chem.*, vol. 14, no. 11, pp. 1347-1363, doi: 10.1002/JCC.540141112.
18. Haghtalab, T., & Soleymanabadi, H. (2016). "Computational studies on chemically engineered carbon nanotubes as HCl sensor," *Indian J. Chem, Sect. A Inorganic, Phys. Theor. Anal. Chem.*, vol. 55A, no. 6, pp. 657-663.
19. Shlaka, J. A., & Abo Nasria, A. H. (2020). "Density functional theory study on the adsorption of AsH_3 gas molecule with monolayer $(AlN)_{21}$ (including pristine, C, B doped and defective aluminium nitride sheet)," *IOP Conf. Ser. Mater. Sci. Eng.*, vol. 928, no. 7, doi: 10.1088/1757-899X/928/7/072082.
20. (2000). The effect of diversity of the nationality, board of director, investment decision, financing decision, and …. . *International Scientific Journal Theoretical & Applied Science*, pp. 311-320, 2000, doi: 10.15863/TAS.
21. Gateaa, Z. A., Abo Nasria, A. H., & Abojassim, A. A. (2021). "Adsorption of gas molecules on (BN) Monolayer as potential SO, SO_2 NO, and NO_2 gases sensor: A DFT study," *Egypt. J. Chem.*, vol. 65, no. 3, pp. 363-374, doi: 10.21608/ejchem.2021.92587.4380.
22. Wang, X. H., et al. (2018). "Effects of adatom and gas molecule adsorption on the physical properties of tellurene: A first principles investigation," *Phys. Chem. Chem. Phys.*, vol. 20, no. 6, pp. 4058-4066, doi: 10.1039/c7cp07906k.
23. Jappor, H. R., Saleh, Z. A., & Abdulsattar, M. A. (2012). "Simulation of electronic structure of aluminum phosphide nanocrystals using ab initio large unit cell method," *Adv. Mater. Sci. Eng.*, vol. 2012, doi: 10.1155/2012/180679.
24. Aghaei, S. M., Monshi, M. M., Torres, I., & Calizo, I. (2017). "Adsorption and dissociation of toxic gas molecules on graphene-like BC3: A search for highly sensitive molecular sensors and catalysts," *arXiv*, no. 2, pp. 1-19.